International Journal of Aeronautical and Space Sciences (2019) 20:518–524
https://doi.org/10.1007/s42405-018-0129-9

ORIGINAL PAPER

Multi-objective Heuristic Design Approach for SAR Mission for Monitoring Local Target Area

Hae-Dong Kim[1] · Jae-Dong Seong[1]

Received: 29 January 2018 / Revised: 7 November 2018 / Accepted: 19 November 2018 / Published online: 8 February 2019

Abstract

The Korea first synthetic aperture radar (SAR) satellite with a 1-m resolution—Korea Multi-purpose Satellite-5 (KOMPSAT-5)—was successfully launched in Korea in 2013, and its successors will be launched continuously to monitor specific target areas. The major requirements of the orbit design for KOMPSAT-5 are that the mean average revisit time (ART) over the Korean peninsula is no longer than 24 h and that the repeat ground track orbit is guaranteed. For this type of problem, an iterative and tedious process may be used to derive the appropriate mission orbit to satisfy the mission requirements. During the design process, sophisticated coverage analysis software should be employed to evaluate the mean ART over a specific local target area. Moccia et al. (Acta Astronaut 47(11):819–829, 2000) presented a feasibility study of a new space-based observation technique using a bistatic SAR and performed a numerical simulation to estimate the measurement accuracy for the bright point target position and velocity. Kim and Chang (Aerosp Sci Technol 40:17–32, 2015) developed an optimal scheduling method employing a genetic algorithm (GA) to reduce the system response time for an SAR satellite constellation. Wei and Chunsheng (Adv Sp Res 50:272–281, 2012) proposed a new design method for a distributed satellite-borne SAR system with an error-propagation model and used a monostatic design to determine the key parameters of a single SAR satellite. Apart from the SAR mission, the orbit design for Earth-observation missions over a specific area or target has been studied by others. Abdelkhlik et al. (J Guid Control Dyn 29(5):1231–1235, 2006) utilized the RGT concept to design natural orbits for visiting a target area without the use of propulsion systems. Kim et al. (J Spacecr Rocket 46(3):725–728, 2009) proposed a new strategy employing a GA to search the current mission orbit for a temporary target orbit to achieve a temporary reconnaissance mission over a particular target site using a low-Earth-orbit satellite during a specific period. We propose an effective approach for the design of the SAR mission for a local target area. Here, the ART and average transmitted power are key parameters for the mission requirements and the bus system, respectively. To our knowledge, no previous studies have considered this kind of problem. To satisfy the mission requirements for the ART over a local target area and simultaneously consider the average transmitted power, multi-objective heuristic algorithms including GEs, particle swarm optimization, and differential evolution are used, and their performances are compared. The computational approach of the design strategy proposed by the authors is based on the optimization algorithms in Matlab® and the powerful coverage analysis tool STK®. Therefore, the proposed strategy is adaptable for various types of SAR mission designs having complex requirements regarding both the orbit and the bus system, particularly for monitoring a specific local target area.

Keywords SAR mission · Genetic algorithm · PSO · DE

Abbreviations

SAR	Synthetic aperture radar
KOMPSAT	Korea multi-purpose satellite
ART	Average revisit time
GA	Genetic algorithm
RGT	Repeat ground track
LEO	Low Earth orbit
PSO	Particle swarm optimization
DE	Differential evolution

✉ Hae-Dong Kim
haedkim@kari.re.kr

[1] Korea Aerospace Research Institute, Daejeon 34133, Republic of Korea

STK	System tool kit
ROI	Region of interest
RAAN	Right ascension of the ascending node
LTAN	Local time of ascending node

1 Optimization Algorithms

The heuristic algorithms are based on experience, regardless of the characteristics of the problem. Indeed, they may provide an effective solution using limited resources, even if the solution is not the global optimum. In this simulation, we used the genetic algorithm, particle swarm optimization, and differential evolution to figure out the best algorithm for orbit-design optimization. Below are the principles of three heuristic algorithms.

Genetic algorithm is based on Darwin's theory of evolution and can solve engineering problems by applying biological evolution mechanism [6]. GA utilized a law of nature stating that suitable individuals for a given environment evolve or die out. The first step is the selection of well-adapted chromosomes, and then, these are mixed to evolve their adaptivity through various crossover methods, with mutation occurring with a low probability to prevent convergence to local minima. The process is iterated until a maximum generation number is reached or a certain tolerance is obtained.

Particle swarm optimization was inspired by the social behavior of animals, such as a flock of birds or a school of fish [7]. The particles are placed in the parameter space of the given problem, and their fitness is evaluated. The movement of the particles is then determined by calculating their velocity, and each particle moves towards the best fitness value by interacting with the other particles. With the addition of some random perturbation, the process is repeated until the maximum generation is reached or a certain tolerance is attained.

Differential evolution is a kind of GA—a solution is iteratively optimized by improving a candidate solution—used for multidimensional real-valued functions [8]. A population of candidate solutions is maintained, and new candidate solutions are created by combining the existing ones according to the simple formula. If nothing is known about the system, the initial population is chosen randomly using a uniform probability distribution. After the functional evaluation, DE generates new parameter vectors by adding a weighted difference vector between two population members to a third member. If the result vectors have lower objective values than the input vectors, the new vectors replace the old ones in subsequent generations. The process is iterated until a maximum generation number is reached or some tolerance level is attained.

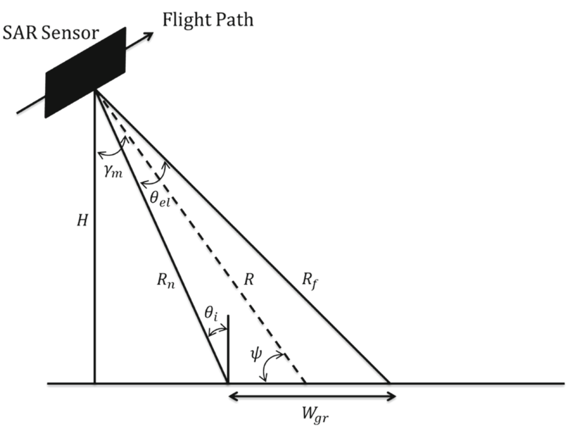

Fig. 1 SAR spaceborne geometry

2 Problem Statement

Our simulation considered a multi-objective optimization in which the target satellite has a sun-synchronous and repeated ground track orbit in an LEO. We performed the simulation in the wide-scan mode, which allows the instantaneous observation of a very broad area with a low resolution.

Figure 1 shows SAR spaceborne geometry. H is the satellite altitude, W_{gr} is the swath, ψ is the grazing angle, γ_{m} is the roll angle of satellite, R is the range between ground and satellite, θ_{i} is the inner incidence angle, and θ_{el} is the elevation beam width.

The goals of our simulation are the minimization of the mean ART and average transmitted power for the SAR sensor. The satellite revisit time indicates the time elapsed between observations of the same point on the ground surface by a satellite, and depends on the orbit of the satellite, the target location, and the swath of the sensor. In this study, the region of interest (ROI) was the Korean peninsula, including Jeju Island, which is the largest island off the coast of Korea. A total of 439 grids (25 km × 25 km) were generated over the ROI. Thus, the mean ART was the average ART among all the grids.

Another major concern of an SAR mission design is the amount of electrical power, which directly affects the size of the solar panels and the capability of the SAR payload. The average transmitter power may vary widely according to the SAR sensor design factors and the satellite mission orbit. The average transmitted power can be calculated as follows [9]:

$$P_{\text{TX-ave}} = \frac{8\pi R^3 \lambda k T_0 F \beta v_{\mathrm{st}} \cos\psi}{\sigma^{\mathrm{o}}_{\mathrm{NE}} A^2 \eta^2 \rho_{\mathrm{r}}}, \tag{1}$$

where R is the middle range, λ is the range operational wavelength, k is the Boltzmann constant (1.381×10^{-23} JK^{-1}), T_0

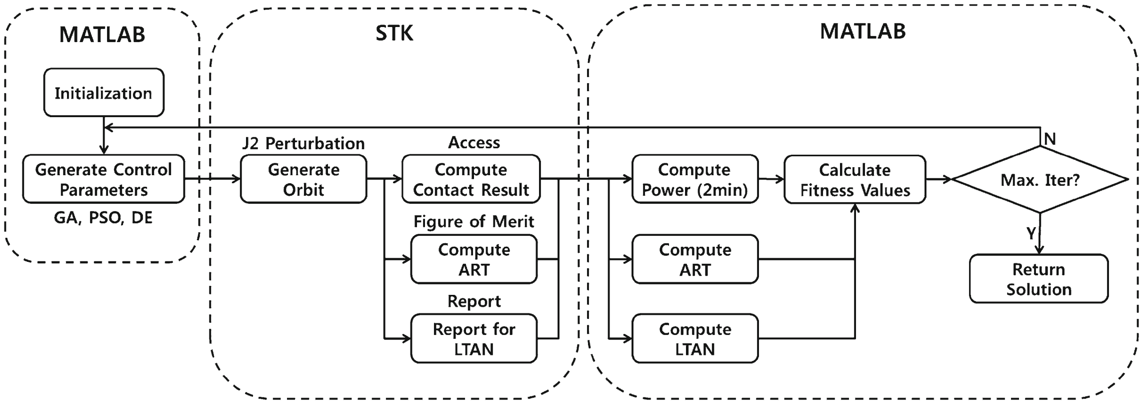

Fig. 2 Flowchart of the proposed approach using STK® and MATLAB®, indicating the three different heuristic algorithms

is the receiver temperature in Kelvin, F is the receiver noise figure, β is the receiving system loss, v_{st} is the velocity of the satellite, ψ is the grazing angle, $\sigma^{\mathrm{o}}_{\mathrm{NE}}$ is the ground radar cross section per unit area, A is the SAR antenna area, η is the antenna efficiency, and ρ_{r} is the slant range resolution.

To achieve the aforementioned goals, we considered four kinds of control parameters in the simulation. The first is the height of the satellite. If the height increases, the satellite requires more average transmitted power, but the ART is shorter. On the other hand, as the height of the satellite decreases, the required average transmitted power decreases, and the ART increases. Thus, in designing the sun-synchronous and repeat ground track orbit, we used the height as a key input parameter for each heuristic algorithm. The second control parameter is the right ascension of the ascending node (RAAN). For SAR satellites, a "dawn-dusk" orbit is generally preferred because of the power supplement for the SAR sensor. The RAAN should be a control parameter for this mission design, as it can affect the ART and the average transmitted power with different orbit tracks and grazing angles. The remaining control parameters are the inner and outer incidence angles, as the SAR sensor cannot provide a high-quality output from the nadir direction. Therefore, we investigate the optimal incidence angles to satisfy the two objectives.

The fitness functions for multi-objective optimization are given as follows:

$$\text{Minimization } f_1 = \frac{\sum_{i=1}^{n} P_i}{n} + w_{\mathrm{p_{dawn}}}, \quad (2)$$

$$\text{Minimization } f_2 = \frac{\sum_{i=1}^{g} T_i}{g} + w_{\mathrm{p_{dawn}}}, \quad (3)$$

where $w_{\mathrm{p_{dawn}}}$ is given as follows:

$$w_{\mathrm{p_{dawn}}} = \begin{cases} 10000 & \text{if LTAN} \notin \pm 10 \text{ min from AM } 06:00 \text{ or PM } 06:00 \\ 0 & \text{if LTAN} \in \pm 10\text{min from AM } 06:00 \text{ or PM } 06:00 \end{cases},$$

and P_i is the average transmitted power for the given ith contact geometry between the satellite and ROI, i.e., the Korean peninsula and Jeju Island; T_i is the ART for the ith grid of the ROI; n is the number of accesses with the ROI; g is the number of grids in the ROI. $w_{\mathrm{p_{dawn}}}$ is the penalty for dissatisfaction of LTAN constraint.

3 Proposed Approach

Figure 2 shows a flowchart of the proposed approach. The control parameters were first generated by each heuristic algorithm, which was implemented in the MATLAB® Optimization Toolbox. Then, a sun-synchronous orbit with a repeated ground track orbit was designed using the height and RAAN input values. The designed orbit parameters were transferred to the J2 propagator through the Active X Interface between MATLAB® and STK®. The main goal of this work is find the reference orbit, so that only J2 perturbation, which is dominant force for LEO satellites, was considered. The other perturbation such as atmosphere drag, third-body attraction, and solar radiation pressure can be compensated by orbit maintenance activities.

In STK®, the access calculation between the satellite and ROI, the ART calculation for each grid of the ROI, and the report generation for the LTAN were performed individually. These STK® results were introduced to the MATLAB® workspace similarly: we calculated two fitness-function values in consideration of the LTAN (dawn-dusk orbit characteristic). These procedures were repeated until the termination condition was obtained. Figure 2 shows a flowchart of the proposed approach employing STK® and MATLAB®, indicating the three different heuristic algorithms.

Table 1 Simulation properties

Item	Value
Analysis time	Until repeat day of designed orbit from 2014.10.01 00:00:00.000
Goals	Minimize ART Minimize average transmitted power
ROI	Korean Peninsula and Jeju Island
Interval between grids	25 km
Control parameters	Height of satellite, RAAN, inner & outer incidence angles of SAR
Constraints	500 km < height of satellite < 600 km 0° < RAAN < 360° 15° < inner incidence angle < 25° (for left and right directions) 45° < outer incidence angle < 55° (for left and right directions) 3 days < number of repeat days < 50 days 05:50 am < LTAN < 06:10 am or 05:50 pm < LTAN < 06:10 pm
Candidate algorithms	GA, PSO, DE

Table 2 Algorithm properties for simulation

Algorithm	Item	Value
All	Population	50
	Generation	200
	Tolerance	1.0e−06
GA	Crossover probability	0.8
	Mutation probability	0.3
	Coding	Binary
	Number of bit	52
PSO	Social factor	2
	Cooperative factor	2
	Nostalgia factor	0.5
	Inertial constant	0.5
	Number of neighbors	5
	Network topology	Star
DE	Scaling-parameter lower boundary	− 1.5
	Scaling-parameter upper boundary	1.5
	Crossover probability	0.95

4 Simulation Results

4.1 Simulation Setup

The properties of the simulation for the orbit-design optimization are presented in Table 1.

The two main objective functions, along with the control parameters and constraints, are presented in Table 1. The analysis start time was October 1, 2014, and the stop time varied according to the repeat day of the designed orbit. A total of 439 grids were used for the ART calculation, with 25-km intervals between them. The large grid number provides more accurate simulation, but simulation time also increases exponentially. Thus, we defined specific number of grid after the trade-off study.

Three simulations were conducted for each of the three algorithms, and a comparison study was performed to determine the best algorithm for the orbit-design optimization. Table 2 shows the properties of the candidate heuristic algorithms. We performed several simulations to find the appropriate properties of optimization algorithms, and consequently, the properties, which are in Table 2, were determined. However, there was no remarkable difference according to specific properties. Through above pre-simulations, we also noticed that the efficiency of algorithm decreased when total calculation number exceeded specific value, and thus, we limited the population and generation number. Approximate calculation time for each simulation was 6 h, but it could be shorter than 6 h when tolerance condition is satisfied.

Table 3 shows the SAR onboard satellite specifications used for the calculation of the average transmitter power. These parameters were provided by KOMPSAT-5, which is an earth-observation satellite with an SAR payload. We suppose that the satellite was operated in the wide-scan mode, which offers a large swath width but a low resolution in the mission-design phase.

Table 3 SAR onboard satellite specification

Item	Value
Frequency	9.65 GHz (X-band)
Range resolution	20 m (wide-scan mode)
Receiver temperature	589 K
Noise figure	4.8 dB
System loss	4 dB
σ^{o}_{NE}	− 26 dB
Antenna width	0.7 m
Antenna length	4.48 m
Antenna efficiency	0.6

The ROI and the satellite with an SAR sensor are shown in Fig. 3.

4.2 Simulation Results

Table 4 summarizes the results of the simulation using the GA. When the GA was used, six non-dominated solutions were generated, all of which achieved dawn-dusk orbit characteristics. The results for the power are distributed in the range of 171–324 W, and those for the ART vary from 21.89 to 30.59 h.

Table 5 presents the results of the simulation using PSO. Eight results were calculated using PSO. The results show the various orbits and heights. The power and ART varied

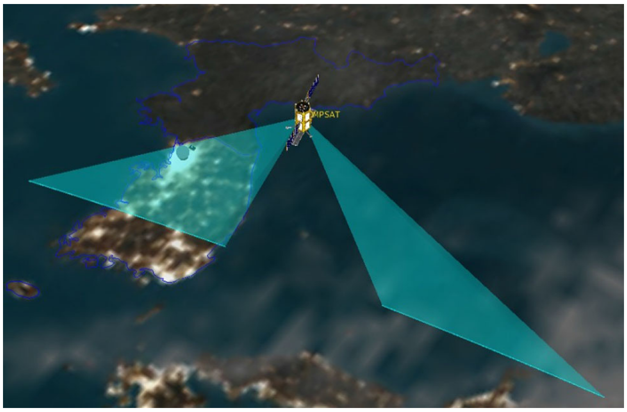

Fig. 3 ROI and satellite with an SAR sensor in the STK® scenario

from 196 to 342 W and 21.05 to 34.7 h, respectively. The results obtained using DE are shown in Table 6.

A total of 19 non-dominated results exhibiting the dawn-dusk orbit were generated using DE. There were only three kinds of orbits. The power and ART varied within the ranges of 124–378 W and 20.28–22.91 h, respectively.

The use of the three algorithms yields the minimization of the average transmitted power and ART, as shown in Fig. 4.

Among the three algorithms, DE had the best performance for this simulation. First, DE revealed the 19 non-dominated solutions, whereas the GA and PSO showed only 6 and 8 of them, respectively. This means that, for the multi-objective optimization, DE offers the user more choices for the overall mission design, increasing the likelihood of a satisfactory design. Second, DE provided the most minimized solutions for the ART. Regarding the ART, the results obtained using DE varied between 20.28 and 22.91 h, which are far lower than the results for the other algorithms. Third, DE converged to a higher value of the outer incidence angle. Unlike the GA and PSO, most of the solutions obtained using DE exhibited a near-maximum value for the outer incidence angle (i.e., 55°). This yields a wider swath and can reduce the ART but increases the average transmitted power. Thus, in Fig. 4, the pareto front of DE indicates a broad distribution of the average transmitted power, because the range between the satellite and ROI increased.

The GA and PSO exhibited lower performances than DE. The results for these two algorithms showed orbit results with various repeat days or counts, and did not present the specific tendency, in contrast to the last characteristic of DE. Therefore, these two algorithms did not converge sufficiently with the given optimization settings, such as the population or generation.

5 Conclusions

In this paper, we proposed a new approach to design an SAR mission for monitoring a local target area considering both

Table 4 Results for GA

	Power (W)	ART (h)	Height (km)	Incidence angle (°)	Number of repeat day (day)	Number of repeat orbit	LTAN
1	171.34	30.59	517.35	18.06–45.92	106	7	06:01:57
2	187.52	27.04	509.94	21.03–50.57	91	6	18:02:28
3	211.70	24.64	509.98	15.68–50.57	91	6	18:02:34
4	221.28	22.36	500.19	15.38–54.56	76	5	06:01:24
5	281.29	22.22	544.08	16.08–54.44	271	18	06:02:35
6	324.14	21.89	581.83	18.22–54.44	224	15	06:01:57

Table 5 Results for PSO

	Power (W)	ART (h)	Height (km)	Incidence angle (°)	Number of repeat day (day)	Number of repeat orbit	LTAN
1	196.16	34.70	501.68	21.47–48.97	547	36	06:02:17
2	198.17	31.48	501.29	20.64–50.75	699	46	06:01:12
3	201.22	31.09	501.68	20.51–50.79	547	36	06:02:30
4	201.42	30.65	502.84	21.27–50.90	319	21	06:02:27
5	203.13	26.65	505.43	18.10–51.44	167	11	06:01:25
6	218.31	25.45	500.16	21.12–51.52	76	5	06:01:12
7	276.13	25.33	528.85	22.49–54.85	287	19	18:02:28
8	342.28	21.05	589.35	15.59–53.51	164	11	18:02:08

Table 6 Results for DE

	Power (W)	ART (h)	Height (km)	Incidence angle (°)	Number of repeat day (day)	Number of repeat orbit	LTAN
1	124.35	22.91	500.25	19.05–52.78	76	5	18:01:18
2	124.56	22.71	500.04	19.44–53.26	76	5	18:01:36
3	124.64	22.60	500.16	19.65–53.47	76	5	18:01:41
4	170.80	22.32	500.12	20.13–54.02	76	5	18:01:16
5	196.99	22.24	500.07	20.03–54.06	76	5	18:01:18
6	200.02	22.23	500.22	19.82–53.92	76	5	18:01:24
7	201.00	22.06	500.14	20.13–54.29	76	5	18:01:18
8	206.86	21.91	500.17	20.28–54.53	76	5	18:01:55
9	209.14	21.64	500.20	20.09–54.69	76	5	18:01:17
10	220.04	21.45	500.17	19.70–54.86	76	5	18:01:37
11	226.08	21.38	500.23	19.63–54.78	76	5	18:01:18
12	232.41	21.35	500.18	19.99–54.87	76	5	18:01:16
13	235.90	21.28	500.18	20.02–54.98	76	5	18:01:40
14	324.81	21.16	578.41	16.36–54.76	269	18	18:02:01
15	325.33	21.16	578.41	16.36–54.77	269	18	18:02:03
16	325.86	20.53	592.31	17.64–54.62	149	10	18:02:03
17	350.62	20.47	592.16	18.02–54.96	149	10	18:02:34
18	351.85	20.28	592.18	17.38–55.00	149	10	18:02:45
19	377.99	20.28	592.30	17.54–54.92	149	10	18:02:49

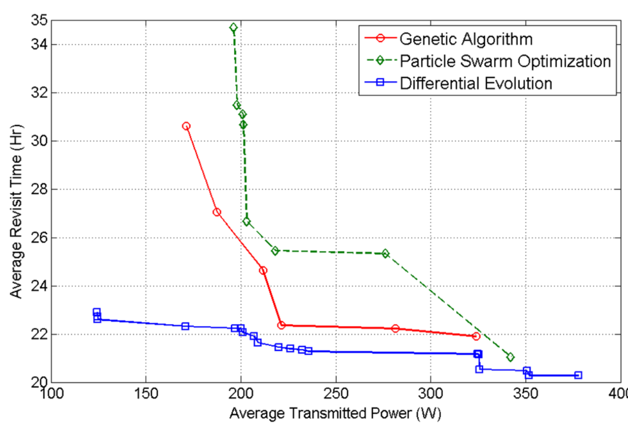

Fig. 4 Pareto front of the simulation

the ART and the average transmitted power. We discuss our preliminary efforts and the results of employing three kinds of heuristic algorithms for this multi-objective problem.

Multi-objective optimization pursues as many as possible candidate solutions while minimizing distance with the utopia solution. It is also very important to get possible candidate solutions during the system-level design phase, because the preliminary design phase can be started with these kinds of several optimized candidate solutions. Thus, we measured the performance of each algorithm in terms of diversity and superiority.

Through a simulation and comparison, the feasibility of the proposed approach was confirmed. The DE algorithm may achieve more efficient results for this kind of problem, whereas analytical approaches may fail to determine an appropriate solution owing to the complex characteristics of the SAR sensor and the key parameters of the satellite over a specific local target area.

Acknowledgements This research was supported by the "A Development of Core Technology for Space Exploration Using Nano-satellite" funded by the Korea Aerospace Research Institute (KARI). We would like to thank KARI for their support.

References

1. Moccia A, Vetrella S, Bertoni R (2000) Mission analysis and design of a bistatic synthetic aperture radar on board a small satellite. Acta Astronaut 47(11):819–829
2. Kim H, Chang Y (2015) Mission scheduling optimization of SAR satellite constellation for minimizing system response time. Aerosp Sci Technol 40:17–32
3. Wei L, Chunsheng L (2012) A novel system parameters design and performance analysis method for distributed satellite-borne SAR system. Adv Sp Res 50:272–281
4. Abdelkhalik O, Mortari D (2006) Orbit design for ground surveillance using genetic algorithms. J Guid Control Dyn 29(5):1231–1235
5. Kim HD, Bang H, Jung OC (2009) Genetic design of target orbits for a temporary reconnaissance mission. J Spacecr Rockets 46(3):725–728

6. Holland J (1975) Adaptation in nature and artificial system. University of Michigan Press, Ann Arbor
7. Kennedy J, Eberhart RC (1995) Particle swarm optimization. In: Proceedings of the IEEE international joint conference on neural networks, Australia, Perth, pp 1942–1948
8. Storn R, Price K (1997) Differential evolution—a simple and efficient heuristic for global optimization over continuous spaces. J Glob Optim 11(4):341–359
9. Bickel DL, Brock BC, Allen CT (1993) Spaceborne SAR study: LDRD 92 final report. Sandia National Laboratories, Albuquerque